Hypersonic flow over spiked cones

By C. J. WOOD

Department of Aeronautics, Imperial College, London University*

(Received 20 September 1961)

An investigation has been made of the flow over spiked cone-cylinders mainly at a Mach number of 10. Five distinct types of flow were discovered. The occurrence of each is defined in terms of spike length and cone angle.

Following a discussion of the flow mechanism, a semi-empirical separation relation is derived. This can be used to predict the flow pattern for the most common type of separated flow.

1. Introduction

With the advent of hypersonic flight, a new interest has arisen in the subject of separated flows. Their use has been envisaged for control purposes, for the reduction of drag and heat transfer and also for variable geometry air intakes.

The phenomenon of flow separation from spikes ahead of blunt axially symmetric bodies has been studied by several investigators at various Mach numbers. In particular, Maull (1960) studied this type of flow at a Mach number of 6·8 and a Reynolds number of $8{\cdot}5 \times 10^4$ based on body diameter. In this work, the emphasis was laid upon the mechanism of the unsteady flow around bodies with short spikes.

The present study began as an extension of that investigation. The object was to study the factors which control the shape and size of the steady separated flow region, in order to provide a basis for the prediction of such flows.

The results obtained by Maull demonstrated the importance of the angular deflexion of the flow at the reattachment point. Consequently, it was decided to use conical bodies in the present investigation, so that the angle between the shear layer and the body surface could be measured easily and varied at will.

2. Apparatus

A detailed description of the Imperial College hypersonic gun tunnel was given by Stollery, Maull & Belcher (1960). For the present work a nozzle extension was fitted, which gave an exit diameter of 4 in. Pitot pressure measurements indicated that the test Mach number increased from 9·2 at the exit to 11 at a station 6 in. downstream (Smith 1961). A value of 10 was taken as the mean Mach number at the position of the model. The stagnation temperature and pressure were approximately 1000 °K and 500 lb./in.^{2} (abs.), respectively, and the Reynolds number was $0{\cdot}7 \times 10^5$ per in.

* Now at the Engineering Laboratory, University of Oxford.

For the general tests, most of the models were $\frac{3}{4}$ in. in diameter, although some early tests were conducted with $\frac{1}{2}$ in. models. The total angles of the conical faces varied from 30° to 180°. They were fitted with steel spikes 0·046 in. in diameter with conical tips approximately $\frac{1}{2}$ in. long. With these spikes, lengths of up to 5 body diameters could be used without vibration.

Special models were also made for specific experiments. In particular, a model was constructed of copper and heated internally by a length of electric fire element to give wall temperatures up to 900 °K. All the other models were at room temperature at the beginning of each test. This was very low compared with the stagnation temperature of the test jet.

Flow visualization was by means of a single-pass schlieren system, using a spark light source. This had a contrast sensitivity of approximately 4000 and a magnification of 0·8.

3. Experimental method

All measurements were made from schlieren photographs by means of a travelling microscope. Because it was never possible to see the actual points of separation and reattachment, their estimated positions were defined in terms of the visible feature of the flow. Thus a consistent system of measurements was introduced. With the assumption that the shear layer was straight, lengths and angles could be calculated, which were geometrically compatible. The major dimensions of the flow pattern were probably accurate to within $\pm 0{\cdot}02$ in. and $\pm \frac{1}{2}$ degree, respectively.

Local flow conditions were found from conical flow charts (Ames research staff 1953). More than 450 photographs were taken in the course of the work in order to reduce the errors caused by the scatter of the results.

4. Results

The principal features of a typical separated flow pattern are sketched in figure 1. This diagram also defines the more important notation to be used later.

The five types of flow

A most striking result of these tests was the discovery of five different types of flow. These occur in regions, which are defined clearly in terms of spike length and cone angle, as shown by figure 2. For convenience, the regions are labelled A to E as shown.

For small cone angles the flow does not separate from the spike. The conical body generates a shock wave, whose angle is the same as if the spike were not present. This type of flow (type A) is shown in figure 3 (plate 1).

As the cone angle is increased beyond the boundary between regions A and B (figure 2), a small region of separated flow appears. The flow separates from the spike and reattaches on the conical face of the body as shown in figure 4 (plate 1).

The size of the separated flow region increases with increasing cone angle, until on the rather ill-defined boundary shown in figure 2, the reattachment point reaches the shoulder of the body. Figure 2 shows that flows of type C with shoulder reattachment (figure 5, plate 1) exist for a wide range of model configurations.

An example of the fourth type of flow is shown in figure 6 (plate 1). This is the oscillatory flow observed by Maull (1960), Mair (1952), Beastall & Turner (1957) and others. It occurs only on bodies with semi-angles greater than the

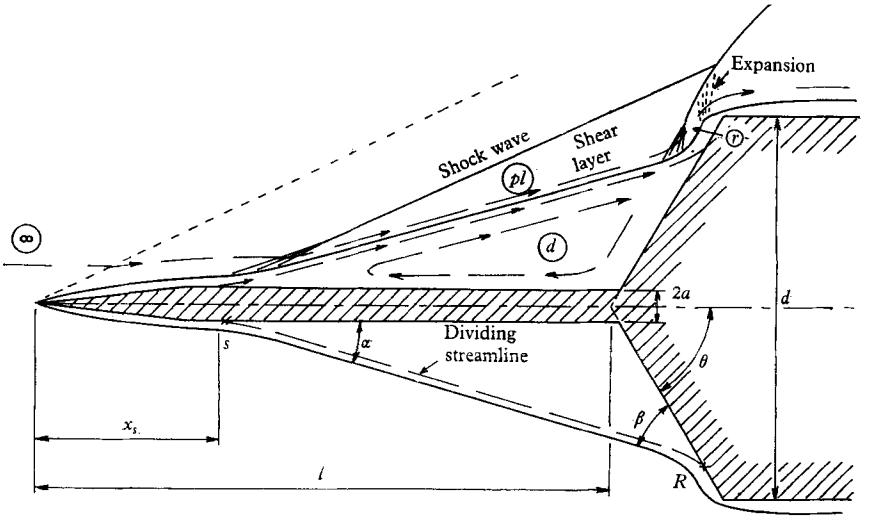

FIGURE 1. Separated flow.

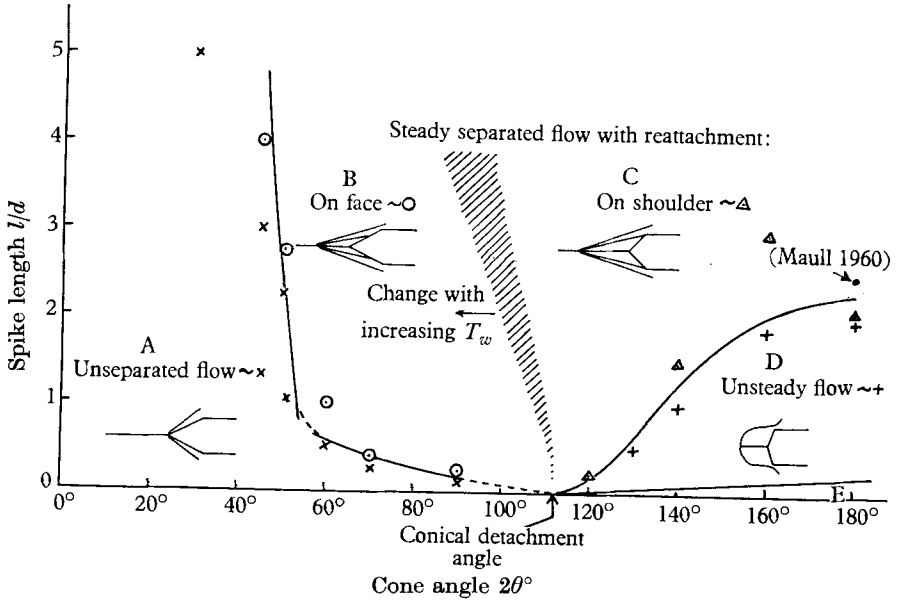

FIGURE 2. Flow regions for spiked cones.
$M_\infty = 10$, $Re_a = 1{\cdot}57 \times 10^3$, $a/d = 0{\cdot}031$, $T_w = 300\,°\mathrm{K}$, $T_\infty = 48\,°\mathrm{K}$.

conical shock detachment angle. The cone angle has a considerable effect upon the amplitude of the oscillation. For angles only slightly greater than the conical detachment angle, the oscillation appears as a ripple in the flow pattern instead of the violent expansion and collapse of the dead air region, which occurs on really blunt bodies.

The last type of flow (type E) is relatively unimportant. It is no different from the flow without a spike, and occurs when the spike is insufficiently long to penetrate the detached shock wave ahead of the body.

An interesting feature of figure 2 is that all the boundaries are centred upon the conical detachment angle. Fully attached flows of type A were never found for cone angles greater than this value. Conversely, oscillatory flow (type D) was never found unless the body alone would have generated a detached shock wave.

The boundary between regions B and C was difficult to determine accurately because of the scatter of the results and the difficulty of judging when the reattachment point reached the shoulder. This boundary was found to be influenced very strongly by the temperature of the body, or rather that of the dead air region. Using the heated model described in § 2, a configuration was found which gave a flow pattern of type B when at room temperature and type C when heated to 810 °K. This effect is shown clearly in figures 7 and 8 (plate 2). It indicates that the size of region C increases considerably at the expense of region B as the temperature of the body increases and approaches the adiabatic recovery temperature. For spiked bodies at normal equilibrium temperatures it appears that most practical separated flows will be of type C. It has been shown that the drag is a minimum for configurations within this region (Church 1960) and it is also clear that this flow pattern protects the greatest possible area of the body surface from the aerodynamic heating associated with attached flow.

All the bodies used in the general tests had sharp shoulders. It was found that varying the shape of the shoulder by means of a small radius or chamfer had a marked effect on the oscillation boundary between regions C and D. Any such modification of the shoulder has a distinct stabilizing effect on the flow. This is consistent with the effect of shoulder radius reported by Maull (1960). Good agreement was obtained with these results despite the difference in Mach number and Reynolds number.

A similar stabilizing effect was found as a result of injecting a small flow of air into the dead air region. On a flat-ended cylinder, a mass injection coefficient $[4\dot{m}(\pi\rho_\infty u_\infty d^2)^{-1}$, where the subscript ∞ refers to undisturbed stream conditions and d is the body diameter] of only 0·08 was sufficient to change the spike length on the oscillation boundary from 2·3 to 1·2 body diameters. This is particularly interesting since Chapman (1949) has suggested that air injection can cause a large reduction in the heat transfer rate at the reattachment point.

The shear layer and the dead air region

A most important feature of all the steady separated flows observed in the present investigation is the fact that the separated shear layers are quite straight for most of their length. This indicates that there are no significant pressure gradients, either along or across the shear layer and that the static pressure in the dead air region is the same as that in the external stream. This absence of significant pressure gradients indicates that the velocities in the dead air region are probably low compared with the velocity of the external stream. Further evidence in support of this conclusion is provided by the fact that spoiler disks

of various sizes, placed in the dead air region, made no difference to the external flow, provided that they did not touch the shear layer (figures 9 and 10, plate 3).

In two-dimensional separated flow at low supersonic speeds, it has been shown that there is a recirculating flow in the dead air region (Mair 1952). The existence of this phenomenon was demonstrated in the present axially symmetric hypersonic case by means of small cotton tufts attached to the spike. Initially these were lying flat and facing the body, but during the run they were lifted by the forward-flowing air near the spike.

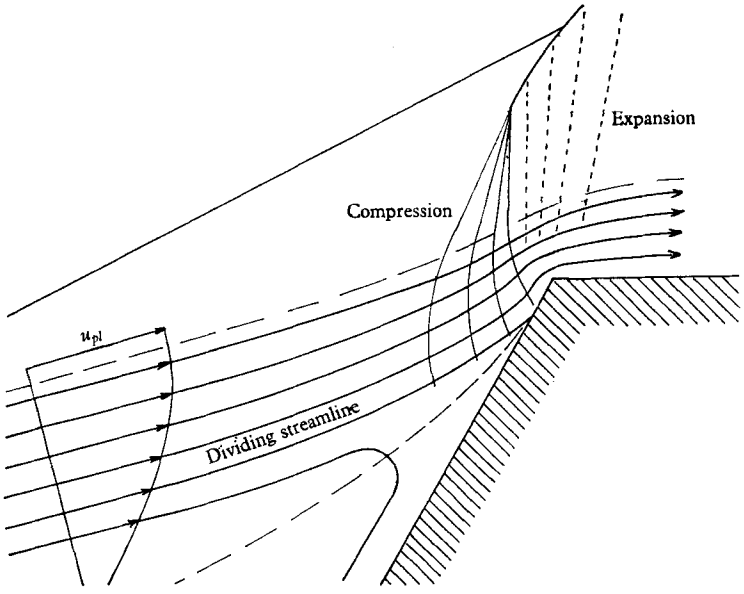

FIGURE 12. Shoulder attachment.

In the case of flows with shoulder reattachment, many photographs showed that the lines representing the shear layer did not touch the body at all (figure 11, plate 3). Nevertheless, a distinct shock wave, generated in this region, showed that the flow was being deflected. Invariably the angle of this shock wave indicated that the flow deflexion was very much less than the geometric reattachment angle β (figure 1).

By simply removing part of the cylindrical portion of the body immediately behind the shoulder, it was proved that the deflexion was caused by the shoulder itself and not by any effect of the boundary layer on the body. Furthermore, an analysis of a typical boundary-layer profile showed that the maximum density gradient occurs near the outer edge. Consequently the line representing a boundary layer or shear layer on a schlieren photograph must also indicate the position of the outer edge.

Thus it was concluded that, although the dividing streamline must always meet the face of the body (§ 6), the outer part of the shear layer may pass outside the shoulder. By this mechanism the deflexion of the external stream and the associated reattachment pressure rise can be very much less than the values required to turn the flow parallel to the face of the body. A sketch of this type of flow is shown in figure 12.

5. The separation relation

There have been several analyses of the separation phenomenon, which have established that the pressure ratio at the separation point is a function of the Mach number and the Reynolds number based on the length of the unseparated boundary layer.

Stratford (1954) established a theoretical model in which the interaction between the boundary layer and an adverse pressure gradient was assumed to affect only a low-velocity sublayer near the wall.

Gadd (1956) used a modified form of this model in two-dimensional supersonic flow. By equating the rate of growth of the sublayer to the deflexion of the external stream, he found a relationship between the pressure coefficient at the

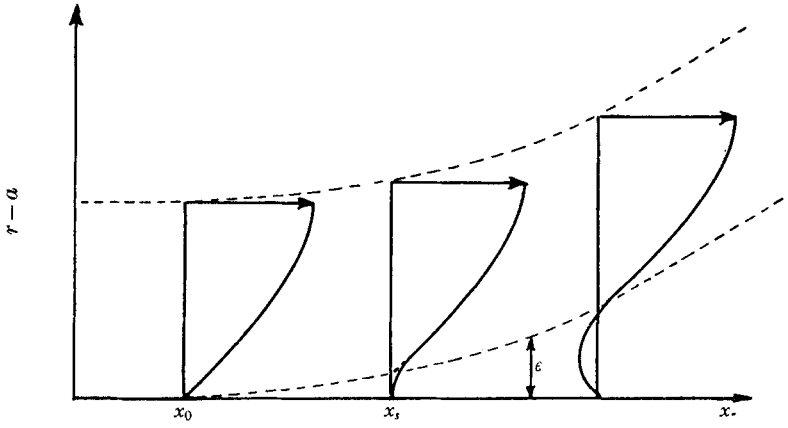

FIGURE 13. Velocity profiles in the interaction region.

separation point and the Mach number and Reynolds number in the external flow. This method included a complicated analysis to determine the velocity profile in the interaction region.

An almost identical model was used by Hakkinen, Greber, Trilling & Abarbanel (1959), who simplified their analysis by assuming that the velocity profile of the undisturbed boundary layer was lifted without distortion by the sublayer, which had a parabolic profile. This mechanism is illustrated in figure 13. It is interesting to note that this method gave a result which was almost identical with that which Gadd obtained for large Reynolds numbers. A similar result was also given by an extremely simple order of magnitude analysis by Chapman, Kuehn & Larson (1957).

The present analysis is based upon the method of Hakkinen *et al.* (1959). It was found that the boundary-layer equations for a thin spike could be reduced to the two-dimensional form if the thickness of the sublayer was assumed to be small compared with the spike radius. This is similar to the normal boundary-layer assumption for axially symmetric flow. However, it is valid for more slender bodies, since the sublayer is already quite thin compared with the boundary layer. Thus it is likely that this method will be reasonably useful in the

present case where the boundary-layer thickness is of the same order as the spike radius. The analysis led to the following result at the separation point:

$$Cf_0 = 2\int_{Cp_s}^{0} f dCp, \tag{1}$$

where Cf_0 is the known skin-friction coefficient in the undisturbed boundary layer just upstream of the interaction region, Cp_s is the separation pressure coefficient based on the same local flow conditions and

$$f(M, Cp(x)) = d\epsilon/dx = \tan\phi(x), \tag{2}$$

where ϵ is the thickness of the sublayer and ϕ is the local deflexion of the external flow.

Using supersonic flow charts (Ames research staff 1953) to obtain the variation of ϕ with Cp in conical flow (tangent-cone approximation), equation (1) was integrated numerically for various Mach numbers. The results were plotted and were found to agree very well with the approximate expression

$$Cf_0 = 2H(Cp_s)^n, \tag{3}$$

where H and n are functions of Mach number only.

To complete the relation, it was necessary to assume an empirical relationship between the separation pressure coefficient and the plateau pressure coefficient Cp_{pl}, which corresponds to the pressure on the straight portion of the separated shear layer. This is in the same form as the expression found by Hakkinen *et al.* for two-dimensional flow: thus

$$Cp_{pl} = KCp_s. \tag{4}$$

Combining equations (3) and (4) led to the final result

$$Cp_{pl} = \frac{K}{2H}(Cf_0)^{1/n}. \tag{5}$$

The values of H and n were given by the numerical integration leading to equation (3). The empirical constant K was then chosen to give the best possible agreement with the experimental separation curve.

The skin-friction coefficient was evaluated from the results of Monaghan (1953) using the Mangler transformation and the first-order transverse curvature correlation of Probstein & Elliot (1956). By this method, the skin-friction distribution was found for the whole spike, including the conical tip. The separation angle was calculated from the pressure coefficient and the results were compared with the experimental data as shown in figure 14. This non-dimensional curve is independent of the shape and size of the body and is valid for a range of geometrically similar spikes at the same Reynolds number based on the spike radius. For a given spike geometry, this may be written in the general form

$$\alpha = g(M, Re_{x_s}, Re_a, x_s/a), \tag{6}$$

where x_s is the distance from the spike tip to the separation point and a is the spike radius.

It was found that good agreement was obtained only if the pressure coefficient was defined in terms of the local flow conditions outside the boundary layer just upstream of the interaction region. Thus the shape of the spike tip, and the self-induced pressures were included. The latter effect was calculated by the approximate method of Talbot, Koga & Sherman (1958). The effect of each of these corrections is shown in figure 14, where it is seen that they are most important. It may also be seen that the experimental points show a marked difference between spikes with ogive tips and those with conical tips, although the diameter was the same in each case. It should be noted that these considerations affect

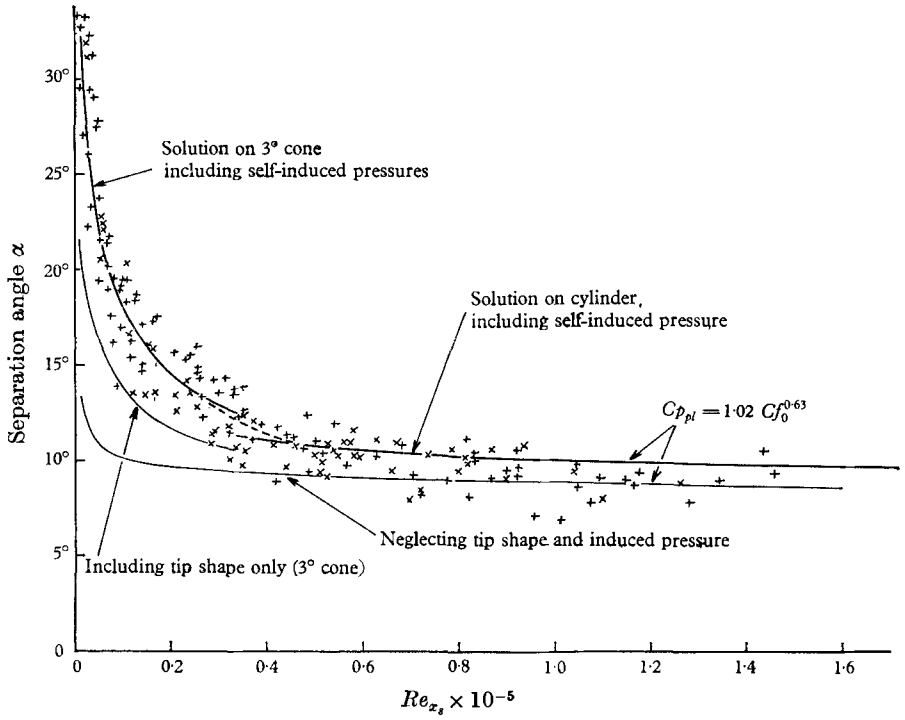

FIGURE 14. Separation curve—the effects of tip shape and self-induced pressure. The operating conditions are $M_\infty = 10$, $Re_a = 1{\cdot}57 \times 10^3$, $T_w = 300\,°\text{K}$, $T_\infty = 48\,°\text{K}$. Results for ogive tips are shown $\times$, for conical tips $+$.

only the shape of the theoretical curve. The choice of the empirical constant K (equation (5)) controls the position as described above. The value of K, which is the ratio of the plateau pressure coefficient to that at the separation point (equation (4)), cannot be determined theoretically without a detailed analysis of the reversed flow region beyond the separation point. By matching experimental and theoretical curves at Mach numbers of 2 (Mair 1952) and at 7 and 10 (present results), K was found to increase with decreasing Mach number, varying between 1 and 4. This is similar to the order of magnitude estimate of Hakkinen *et al.* and is consistent with the obvious requirement that the plateau pressure should be somewhat higher than the separation pressure (equation (4)). Thus the value of K provides some indication that the present method of analysis gives reasonable results.

Tests with varying spike radii showed that the method overestimates the effect of transverse curvature. However, this is a small effect and the error should not be important. The theoretical results also show a slight increase in the separation angle with increasing spike temperature whereas the experimental results show no visible trend.

It is interesting to note that the 'incipient separation' boundary between the regions A and B in figure 2 is related to the separation curve by the simple expression

$$Cp_{is} = 6Cp_{pl}. \tag{7}$$

As shown in § 4, this boundary corresponds to the condition when the fully attached boundary layer is just about to separate.

6. The reattachment relation

The work of Chapman *et al.* (1957) has provided a valuable explanation of the flow mechanism at the reattachment point. In steady separated flows there must be a fixed mass of fluid in the dead air region. This is enclosed by the dividing streamline, which joins the stagnation points at separation and reattachment. For equilibrium, the pressure rise required to bring the dividing streamline to a stagnation point on the surface of the body must correspond to the deflexion of the external supersonic stream. In the case of flows which reattach on a large flat surface, this deflexion is equal to the geometrical reattachment angle between the shear layer and the surface. However, in the present case the flow pattern is complicated by the proximity of the body shoulder, where the sudden expansion exerts a considerable upstream influence in the boundary layer. Consequently it is impossible to make a quantitative estimate of the flow deflexion. However, it is clear that the deflexion and the associated pressure rise will decrease as the reattachment point approaches the shoulder. This decrease will become very steep at the shoulder itself, as a result of the partial reattachment mechanism described in § 4.

Since the flow deflexion varies in this way with reattachment position, it is possible for the reattachment point to move until the required pressure rise is achieved. Thus, as the cone angle is increased, the reattachment point moves towards the shoulder to maintain the equilibrium. This movement is checked at the shoulder, where a large variation in the pressure rise can occur with a negligible change in the flow pattern. These conclusions are verified by the general trend of the experimental results (figure 2).

Although it is not possible in the present case to calculate the deflexion of the external stream, it is possible to estimate the pressure rise required to bring the dividing streamline to a stagnation point. The general method has been described by Chapman *et al.* (1957). In the present case it is modified to include the effects of heat transfer.

If it is assumed that the dividing streamline suffers an isentropic compression near the reattachment point, then the pressure p_r at that point is related to the plateau pressure p_{pl} by

$$\frac{p_r}{p_{pl}} = \{1 + (\gamma - 1)\,\bar{M}^2\}^{\gamma/(\gamma-1)}, \tag{8}$$

where $\bar{M}$ is the Mach number on the dividing streamline. This Mach number can be related to the velocity $\bar{u}$ by an expression which is derived from the Crocco integral of the energy equation. Substituting this expression in equation (8) leads to the following result for the pressure ratio, where T is the absolute temperature. The suffices d and pl refer to conditions in the separated region and just outside the shear layer, respectively.

$$\frac{p_r}{p_{pl}} = \left\{ \frac{[T_d(1-u')/T_{pl}] + \frac{1}{2}(\gamma-1)\,M_{pl}^2 u' + u'}{[T_d(1-u')/T_{pl}] + \frac{1}{2}(\gamma-1)\,M_{pl}^2 u'(1-u') + u'} \right\}^{\gamma/(\gamma-1)}, \tag{9}$$

where

$$u' = \bar{u}/u_{pl}. \tag{10}$$

Applying the Mangler transformation in the relatively thin conical shear layer, it is found that the laminar mixing result of Chapman (1949) holds for conical separated flows, where there is no boundary layer upstream of the separation point. In the present case u' is zero at the separation point and approaches the Chapman value of 0·587 asymptotically in the streamwise direction. This conclusion is supported by the work of Nash (1960) and Glick (1960). Using the Chapman result, which is independent of Mach number and temperature, the maximum reattachment pressure rise can be calculated from equation (9). This alone is not sufficient to predict the position of the reattachment point, but it does lead to an interesting and quite unexpected conclusion.

The form of equation (9) shows at once that the temperature of the dead air region T_d is a most important parameter in the calculation of the reattachment conditions. Bearing in mind that $u' < 1$, it is seen that the pressure ratio will decrease as T_d increases. A comparison between this result and the experimental effect of dead air temperature, described in § 4, provides a striking confirmation of the reattachment mechanism described in this section. Figures 7 and 8 (plate 2) show that an increase in the dead air temperature, which has been shown to correspond to a decrease in the required reattachment pressure rise, actually results in an outward movement of the reattachment point.

A further important conclusion may be drawn from these results. The way in which the dead air temperature affects the overall flow pattern makes it quite clear that it is the flow at the reattachment point which controls the shape and size of the dead air region. The straight shear layer simply moves according to the unique separation relation described in § 5, until the reattachment condition is satisfied.

With flows of type C, this mechanism enables the flow pattern to be predicted without any reference to the flow at the reattachment point. Since this point is fixed on the body shoulder, the problem is reduced to a simple geometric relationship between the separation angle and the position of the separation point. With the notation of figure 1, this may be written

$$\tfrac{1}{2} - (a/d) = \{(l/d) + \tfrac{1}{2}\cot\theta - (x_s/d)\}\tan\alpha. \tag{11}$$

The flow pattern may be determined by the simultaneous solution of this relationship and the separation relation expressed in equation (6).

7. Conclusions

This investigation has shown that the shape and size of a region of separated flow is controlled primarily by the flow near the reattachment point, where the dividing streamline is brought to rest by the reattachment pressure rise. At the separation point there is a relation between the separation angle and the spike length ahead of separation. This relation is independent of the shape and size of the body. It is a function of the Mach number, Reynolds number and spike geometry, with a negligible effect of spike temperature. The position of the straight shear layer adjusts itself according to the separation relation, until the reattachment condition is satisfied.

This mechanism causes the formation of four main types of flow. One of these is of particular interest in that the reattachment point remains close to the shoulder of the body. Consequently, this type of flow gives the greatest possible reduction of drag and heat transfer. A further advantage is that the flow pattern can be predicted easily by means of the separation relation and the geometry of the model.

The oscillatory type of flow, which has attracted considerable interest, is also found on conical spiked bodies, provided that the angle of the cone is greater than the conical detachment angle.

In addition to these positive conclusions, the present investigation has demonstrated the need for a detailed investigation of the flow in the dead air region and of the mechanism of reattachment near an expansion corner.

This paper is an abridged form of the thesis submitted for the degree of Doctor of Philosophy in the University of London.

REFERENCES

AMES RESEARCH STAFF 1953 *Nat. Adv. Comm. Aero., Wash., Tech. Rep.* no. 1135.

BEASTALL, D. & TURNER, J. 1957 *Aero. Res. Counc., Lond., Rep. & Mem.* no. 3007.

CHAPMAN, D. R. 1949 *Nat. Adv. Comm. Aero., Wash., Tech. Note,* no. 1800.

CHAPMAN, D. R. 1956 *Nat. Adv. Comm. Aero., Wash., Tech. Note,* no. 3792.

CHAPMAN, D. R., KUEHN, D. M. & LARSON, H. K. 1957 *Nat. Adv. Comm. Aero., Wash., Tech. Note,* no. 3869.

CHURCH, P. D. 1960 *J. C. Guilds Engng Soc.* (Imperial College), **11**, 29.

GADD, G. E. 1956 *Aero. Res. Counc., Lond., Rep.* no. 18,494.

GLICK, H. S. 1960 *Cal. Tech. Hypersonic Research Project, Memo.* no. 53.

HAKKINEN, R. J., GREBER, I., TRILLING, L. & ABARBANEL, S. S. 1959 *Nat. Aero/Space Admin. Memo.* 2/18/59W (T.I.L. 6276).

MAIR, W. A. 1952 *Aero. Res. Counc., Lond., Rep.* no. 14,712.

MAULL, D. J. 1960 *J. Fluid Mech.* **8**, 584.

MONAGHAN, R. J. 1953 *Aero. Res. Counc., Lond., Rep. & Mem.* no. 2760.

NASH, J. F. 1960 *Aero. Res. Counc., Lond., Rep.* no. 22,245.

PROBSTEIN, R. F. & ELLIOT, D. 1956 *J. Aero/Space Sci.* **23**, 208.

SMITH, J. E. Private communication.

STOLLERY, J. L., MAULL, D. J. & BELCHER, B. J. 1960 *J. Roy. Aero. Soc.* **64**, 24.

STRATFORD, B. S. 1954 *Aero. Res. Counc., Lond., Rep. & Mem.* no. 3002.

TALBOT, L., KOGA, T. & SHERMAN, P. M. 1958 *Nat. Adv. Comm. Aero., Wash., Tech. Note* no. 4327.

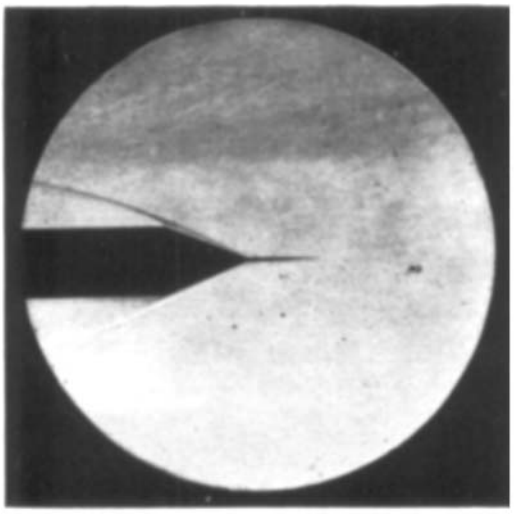

FIGURE 3. Unseparated flow (type A).

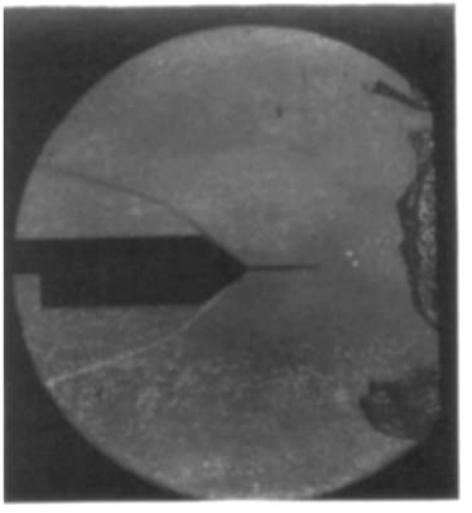

FIGURE 4. Separated flow (type B).

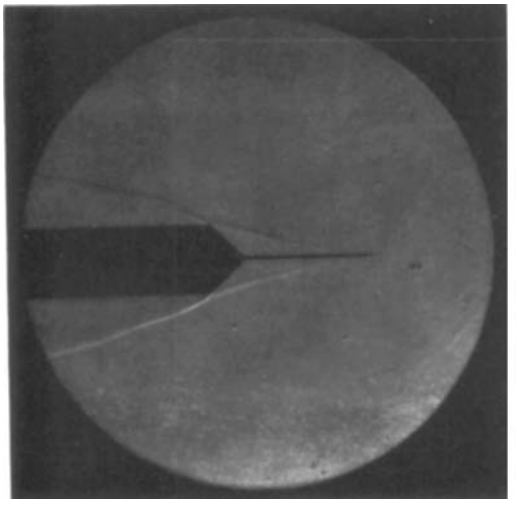

FIGURE 5. Separated flow (type C).

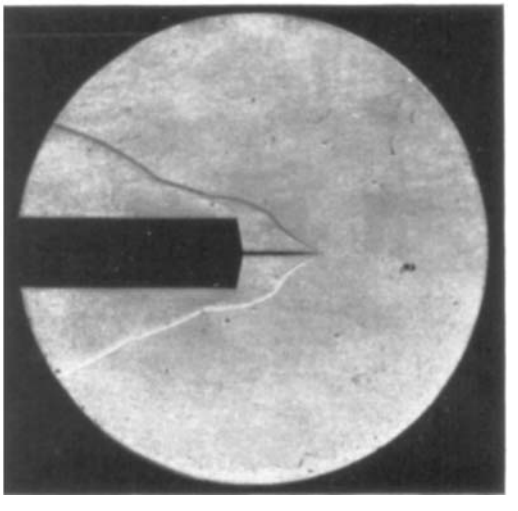

FIGURE 6. Oscillatory flow (type D).

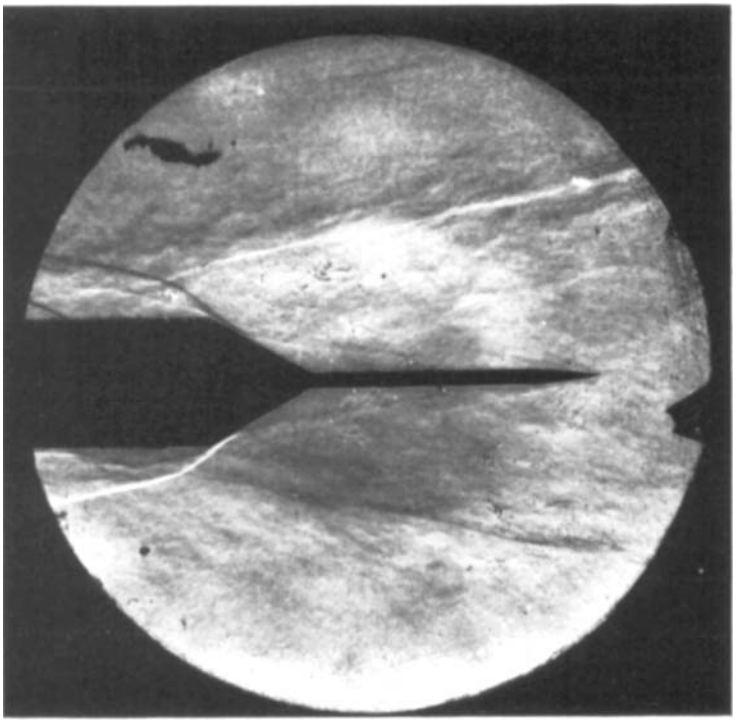

FIGURE 7. Model at 300°K.

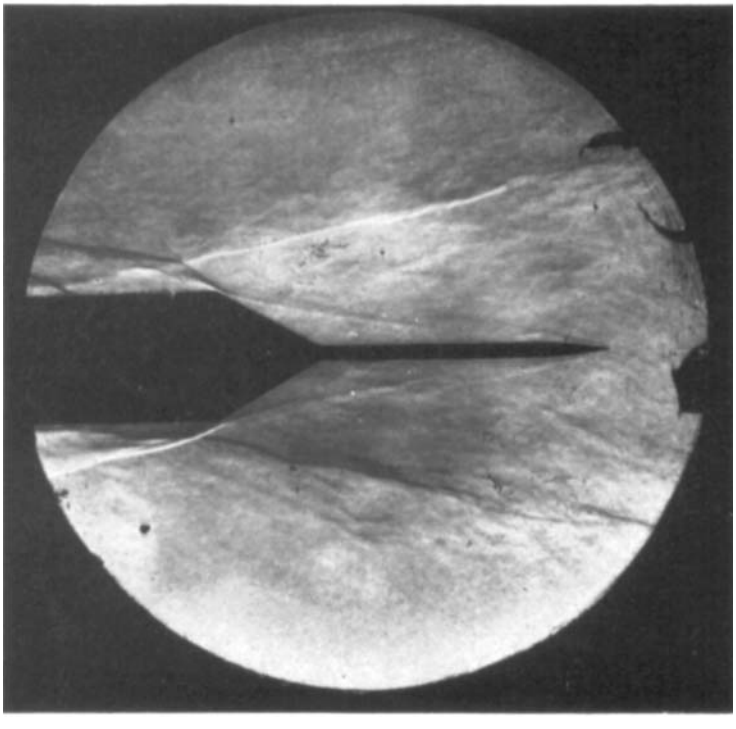

FIGURE 8. Model at 810°K.

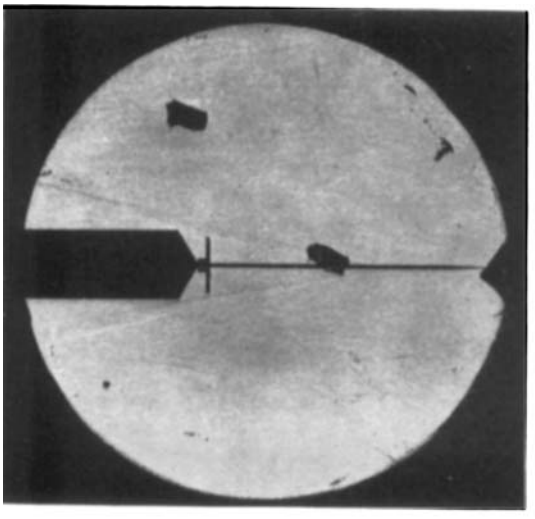

FIGURE 9. Flow with spoiler disk.

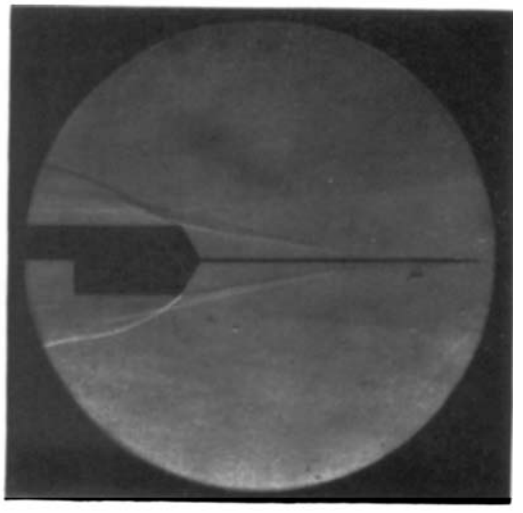

FIGURE 10. Flow without spoiler disk.

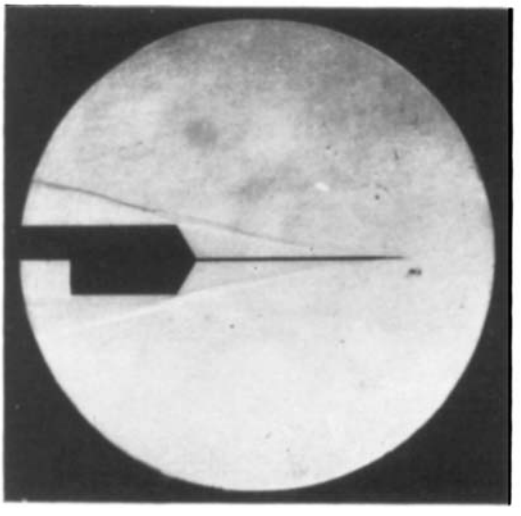

FIGURE 11. Shoulder reattachment.